Technical Note

Integrated Borehole GPR and Optical Imaging for Field Investigation of Rock Mass Structures

Yangyang Xiong , Haijun Chen , Zengqiang Han * , Chao Wang

Posted Date: 27 March 2026

doi: 10.20944/preprints202603.2238.v1

Keywords: borehole optical imaging; borehole GPR; dielectric constant; dynamic exploration method; rock mass structures

 doi:10.20944/preprints202603.2238.v1

Technical Note

Integrated Borehole GPR and Optical Imaging for Field Investigation of Rock Mass Structures

Yangyang Xiong [1,2], Haijun Chen [1,2], Zengqiang Han [3,*] and Chao Wang [3]

[1] China Railway Tunnel Consultants Co., Ltd., Guangzhou 511458, China
[2] Key Laboratory of Intelligent Monitoring and Maintenance of Tunnel Structure, CRTG, Guangzhou 511458, China
[3] State Key Laboratory of Geomechanics and Geotechnical Engineering Safety, Institute of Rock and Soil Mechanics, Chinese Academy of Sciences, Wuhan 430071, China
* Correspondence: zqhan@whrsm.ac.cn

Abstract

Conventional drilling and coring methods are inherently limited to providing one-dimensional geological data, which hinders accurate characterization of the spatial distribution of rock mass structures and properties. Mechanical disturbances during drilling often cause core breakage, further compromising the fidelity of in-situ geological representation. This study proposes an integrated approach combining borehole optical imaging and ground-penetrating radar (GPR) for enhanced characterization of rock mass structures. A dynamic exploration methodology is introduced, defined as an adaptive drilling layout workflow based on phased information feedback. The fundamental concept, key assumptions, boundary conditions, and field implementation procedures of this dynamic survey are systematically described. The integrated method was applied to a high-speed railway investigation project in the Tengzhou section, Shandong Province, China, where six boreholes were surveyed using both techniques. Results demonstrate that fused analysis of borehole optical images and GPR data effectively reveals rock morphology, fracture distribution, joint systems, fractured zones, and geological features such as rock veins. The method's complementary strengths—optical imaging providing high-resolution orientation data at the borehole wall and GPR extending detection radially into the surrounding rock mass—enable spatially enhanced characterization while partially mitigating the azimuthal ambiguity inherent in single-borehole radar measurements. A triangular borehole survey scheme is shown to be feasible for locating subsurface anomalies. The proposed dynamic exploration method effectively reduces borehole requirements compared to conventional grid layouts while successfully identifying common anomalous features through integrated analysis of optical imaging and GPR data. The method demonstrates practical applicability for detecting fractures with apertures greater than 1 cm and meter-scale cavities, with good consistency between the two techniques validating the feasibility of this integrated approach. The method's limitations, including resolution constraints and detection omission risks, are explicitly acknowledged, and risk control strategies are proposed. Overall, the dynamic exploration approach reduces investigation costs, accelerates project time-lines, and provides a practical framework for spatial characterization of rock mass discontinuities with minimal borehole requirements.

Keywords: borehole optical imaging; borehole GPR; dielectric constant; dynamic exploration method; rock mass structures

1. Introduction

Drilling is a fundamental method in geological investigation, widely employed across various engineering projects to obtain subsurface rock and soil samples, understand geological conditions, and assess rock mass quality. However, due to the inherent complexity and uniqueness of geological environments, evaluating rock mass quality based solely on drilling and coring presents significant

 doi:10.20944/preprints202603.2238.v1

limitations. Conventional drilling and coring techniques are inherently one-dimensional and susceptible to mechanical disturbances during sampling, often resulting in core breakage and low recovery rates. Furthermore, drill cores provide information only along the borehole axis, offering limited insight into the surrounding rock mass. A comprehensive understanding of site geology typically requires extensive drilling, yet conventional programs lack the flexibility for real-time adjustment based on field conditions. Consequently, there is a growing demand for efficient, accurate, and integrated exploration technologies capable of addressing engineering geo-logical problems economically and effectively.

Borehole optical imaging systems, developed on the basis of digital and panoramic technologies, have become essential tools in geological exploration [1–3]. These systems enable direct visual observation of borehole walls, generating high-resolution images that provide complete records of geological features—including fracture orientation, aperture width, and other geometric parameters—thereby addressing the limitations of traditional core-based methods in terms of completeness and accuracy. Borehole optical imaging is particularly valuable in operations with low core recovery rates, significantly enhancing both the technical standard and precision of engineering geological surveys.

Borehole Ground Penetrating Radar (GPR) is a technique that extends GPR surveys into boreholes [4–6]. By directly accessing deeper subsurface regions, it combines the high-resolution advantages of surface GPR with the depth penetration enabled by boreholes. Borehole GPR serves as an effective means for obtaining two-dimensional information about the rock mass surrounding the borehole and can detect features beyond the borehole wall.

Numerous studies have explored the application of these two technologies in geological structure investigation. Li et al. (2013) [7] proposed an ISRM Suggested Method for rock fracture observation using a digital optical televiewer, applicable in both air- and fluid-filled boreholes. Kevin J. et al. (2004) [8] integrated GPR, optical borehole images, and core data to characterize porosity, hydraulic conductivity, and paleokarst features. Zhong et al. (2011) [9] introduced an integrated exploration method combining borehole GPR and borehole imaging for rapid identification of geological structures. Thomas et al. (2007) [10] characterized unstable rock masses using borehole logs and diverse GPR data. Williams and Johnson (2004) [11] investigated fractured-rock aquifers using acoustic and optical borehole-wall imaging, concluding that integrated interpretation of multiple methods yields the most robust results. Serzu et al. (2004) [12] employed borehole GPR to characterize fractures in granitic bedrock. Li et al. (2021) [13] analyzed single-hole reflection imaging principles, validating GPR image patterns with optical borehole images.

While these studies have advanced the individual applications of borehole optical imaging and GPR, several critical gaps remain. First, although the complementary nature of these techniques is widely acknowledged [14–18], a systematic framework for their deep integration—beyond qualitative comparison—has yet to be established. Second, single borehole GPR data inherently suffer from azimuthal ambiguity, as conventional dipole antennas transmit and receive signals over a full 360° range without directional information. Optical imaging can precisely orient fractures intersecting the borehole wall, but cannot resolve the azimuthal ambiguity of radar reflections from features that do not intersect the borehole. This dimensional incompatibility—optical data providing orientation at a point, single-hole GPR providing range without bearing—has not been adequately addressed in existing fusion approaches. Third, existing methods for estimating dielectric permittivity from borehole GPR data often rely on simplified assumptions (e.g., point-source reflections, homogeneous media) that do not account for frequency-dependent dispersion, full-waveform characteristics, or the complex petrophysical factors controlling radar reflections (e.g., fracture aperture relative to wave-length, fluid saturation and salinity, clay mineral content). Fourth, most previous studies have focused on either single-hole analysis or qualitative correlation, lacking an adaptive decision-making framework that optimizes borehole placement based on real-time data feedback to minimize drilling while maximizing information yield.

 doi:10.20944/preprints202603.2238.v1

To address these gaps, this paper proposes a dynamic exploration methodology that integrates borehole optical imaging and GPR within an adaptive drilling framework. The key innovations of this study are threefold:

(1) Methodological innovation: We develop a feedback-based adaptive borehole layout workflow—termed dynamic exploration—that adjusts drilling locations in real time based on preliminary findings, enabling efficient delineation of unfavorable geological bodies (e.g., fractures, cavities, karst zones) with minimal borehole requirements.

(2) Technical innovation: We establish a novel approach for estimating relative dielectric permittivity by jointly analyzing the slope of radar echo curves (derived from GPR profiles) and fracture orientation data (derived from optical images). This method provides an alternative means for velocity model construction, partially addressing the limitations of conventional single-method dielectric estimates.

(3) Applied innovation: For the first time, we systematically apply the integrated borehole optical imaging and GPR method to high-speed railway engineering investigation, demonstrating its feasibility and effectiveness through measured data from six boreholes in the Tengzhou section of the Jinghu high-speed railway project.

Three key questions guide the investigation: (1) How can the fusion of borehole optical imaging and GPR data compensate for the azimuthal ambiguity inherent in single-borehole radar measurements? (2) Can the joint use of reflection curve geometry and optical fracture orientation improve the accuracy of dielectric constant estimation and, consequently, velocity modeling? (3) Can a dynamic exploration approach based on a limited number of boreholes effectively identify and locate subsurface anomalies of engineering concern? By addressing these questions, a practical and scientifically grounded framework is established for the spatial characterization of rock mass discontinuities with minimal borehole requirements, responding to a critical need in engineering geological exploration.

2. Materials and Methods

2.1. Borehole GPR

Borehole GPR is a kind of broad-spectrum electromagnetic technology to determine the distribution of underground media. It can penetrate a certain distance in geotechnical media, and the frequency used is usually 50-250 MHz. The principle of borehole GPR is the same as that of GPR used on the ground. One antenna is used to transmit high-frequency broadband electromagnetic waves, and the other antenna receives the transmitted waves from the underground geotechnical medium. The propagation of the radar wave is affected by the electromagnetic properties and geometric forms of rock and soil, and the electromagnetic wave strength and waveform at the receiving end will change accordingly. According to the Travel Time, Amplitude, and Waveform data of the electromagnetic wave at the receiving end, the structural characteristics of the underground geotechnical medium can be inferred.

In the single hole reflection measurement mode, the radar transmitting antenna and receiving antenna are placed in the same borehole at a fixed spacing, and the spacing is fixed. The optical cable used for signal transmission, trigger, and data acquisition can eliminate the additional interference of ordinary cables to the receiving and transmitting antennas. The common antenna of the borehole GPR is a dipole antenna, which can radiate and receive signals from 360° space. As with the ground penetrating radar, the interpretation of the borehole GPR is to determine the geological characteristics of the reflection wave group according to the waveform and intensity characteristics of the reflection wave group in the geological radar image profile obtained after data processing and through the tracking of the same phase axis. When there are unfavorable geological bodies in the rock mass (such as fractures, bedding, fracture zones, karst, and groundwater, etc.), the electrical properties of the unfavorable geological bodies are quite different from those of the surrounding rock masses, which makes it easy to form strong reflection waves. At the same time, the diffracted waves may also be

 doi:10.20944/preprints202603.2238.v1

generated due to the differences in lithology, forming a hyperbolic feature on the time profile. The difference between the interpretation of borehole radar mainly lies in the interpretation of space. For common GPR, all the reflections come from half space, while for borehole GPR, the reflections come from the 360° radial range. In general, it is difficult to determine the reflector's azimuth using the single-borehole GPR data, but only the reflector's distance can be determined. When the reflector is plane, the included angle between the plane and the borehole can also be determined. For point targets, the reflection signal is hyperbolic, and for fractures that do not pass through the borehole, the reflection signal is oblique, as shown in Figure 1. The angle between the oblique line and the borehole is determined by the angle between the crack and the borehole. When the fracture passes through the borehole, the reflection characteristics are like open scissors, and the fracture shape can be inferred from these characteristics.

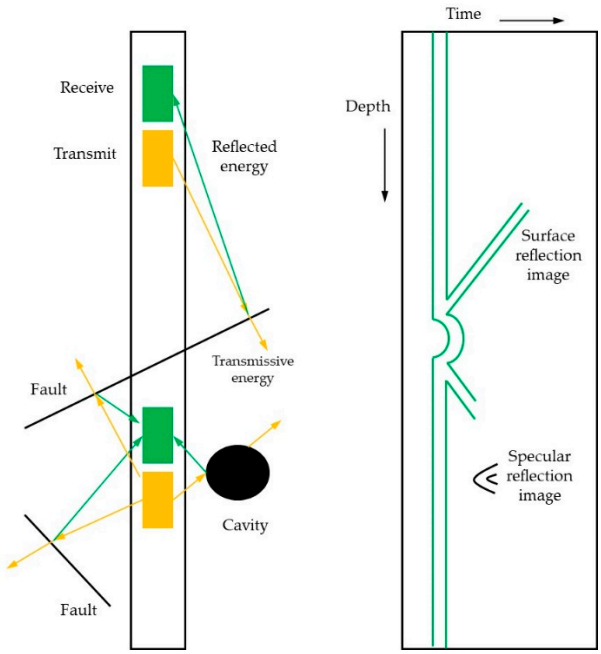

Figure 1. Antenna arrangement of radar single hole reflection measurement and radar image sketch of rock fault and cavity.

Antenna arrangement of radar single hole reflection measurement and radar images of faults and cavities in rock mass are shown. The figure intuitively shows the reflection and transmission of radar wave signals by three typical unfavorable geological bodies, namely, cavities, faults passing through boreholes, and faults not passing through boreholes, and gives their typical reflection radar profiles.

2.2. Borehole Optical Imaging

The key of digital panoramic borehole camera system is the breakthrough of panoramic technology (truncated cone reflector) and digital technology (digital video and digital image). Panoramic technology realizes the two-dimensional representation of a 360° borehole wall, and the plane image formed after superimposing the azimuth information is called a panoramic image; digital technology realizes the digitalization of the video image. Through the inverse conversion of a panoramic image, the real borehole wall is restored to form a digital columnar image of the borehole wall.

The digital panoramic borehole camera system uses a cone mirror, and the hole wall image is deformed after being reflected by the cone mirror. It is necessary to understand the change rule of plane fractures in the panoramic image to improve the on-site monitoring level. The process of digital

 doi:10.20944/preprints202603.2238.v1

borehole camera testing is essentially a process of reconstructing the cylindrical surface of the borehole wall through processing after the borehole wall is photographed and recorded by the probe. A conical mirror only reflects a section of the wall, and cracks with a large longitudinal length need to be displayed by multiple images. The process from the bottom of the cone mirror to the top of the crack and beyond the lowest point is also the process in which the highest point of the crack in the panoramic image enters the outer circle from the opposite direction of the tendency, and each point gradually appears in the circle, and the lowest point of the crack leaves the inner circle in the direction of the tendency of the crack. The crack in the panoramic image is the projection of the space crack on the conical mirror. The whole wall in the panoramic image is a circle; the inner circle is the upper end of the wall, and the outer circle is the lower end. The position of the point on the hole wall in the circle is related to the azimuth of the point. For example, point A in the right west direction appears at 270° in the panoramic image as shown in Figure 2. The movement mode of the point on the hole wall in the continuous multi-frame panoramic image is: enter the outer circle → move to the inner circle along the radial direction → move out of the inner circle. In the panoramic image, horizontal fractures are concentric circles, vertical fractures are radial line segments, and oblique fractures are conic curves.

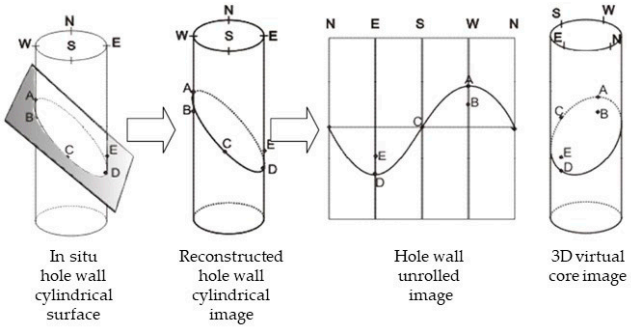

Figure 2. The changing appearance of the fracture in the panoramic image.

The apparatus of borehole optical imaging mainly consists of the probe, depth measuring device, integrating control box, winch, and cables, as shown in the Figure 3.

Figure 3. The basic components of a typical borehole digital optical camera system.

2.3. Comparison of Borehole GPR and Borehole Optical Imaging Data

To ensure the clarity and scientific rigor of the proposed methodology, this section explicitly outlines the basic assumptions and boundary conditions that underpin the integrated approach combining borehole optical imaging and GPR.

Basic Assumptions:

 doi:10.20944/preprints202603.2238.v1

(1) The rock mass is treated as an isotropic or weakly anisotropic medium, and the electromagnetic wave velocity is assumed to be approximately constant within local regions. This assumption enables simplified velocity modeling for GPR data interpretation.

(2) Structural planes (e.g., fractures, bedding planes) are approximated as smooth surfaces. This simplification is adopted specifically for geometric orientation estimation (dip angle and dip direction) from optical images and radar reflection patterns. It is important to note that this assumption is not suitable for mechanical parameter analysis (e.g., shear strength) where surface roughness plays a critical role.

(3) The dielectric properties of fracture infill materials (e.g., air, water, clay) differ significantly from those of the surrounding rock matrix, enabling detectable radar reflections. This contrast is essential for identifying fractures and cavities in GPR profiles.

(4) The depth positioning of borehole optical imaging and radar detection is consistent, allowing for accurate data fusion. This is achieved through synchronized depth recording during field data acquisition.

Boundary Conditions:

(1) The applicable borehole diameter ranges from Φ46 to Φ130 mm, and the borehole conditions require clear water or dry hole environments. Turbid water or mud-filled boreholes may compromise optical image quality and are therefore excluded from the method's applicability.

(2) The GPR operating frequency is 50-250 MHz, which is suitable for detecting geological structures at the meter scale. Consequently, the proposed method is applicable to fractures with apertures greater than approximately 1 cm and cavities within the detectable range of borehole GPR. The method is not suitable for detecting sub-centimeter scale fractures that fall below the resolution limits of GPR.

There are many correlations between the structure of the borehole radar and the borehole camera. Cracks, cavities, metals, surface disturbances, etc., can be characterized by their respective images in optical images and radar images. For example, the optical drilling image can clearly reflect the trace occurrence of the crack on the hole wall profile, while the drilling radar profile shows an open scissors-like echo curve at the same depth, and can reflect the possible extension area of the crack, as shown in Figure 4. Because the dielectric properties of the upper and lower media differ greatly, the soil-rock interface will also produce significantly different radar echo characteristics above and below the interface. In addition, because the aquifer, clay layer, and metal objects have obvious absorption and attenuation effects on the radar wave, the echo signal is also weak when encountering these media. For the section with a metal casing in the hole, there is almost no significant echo signal.

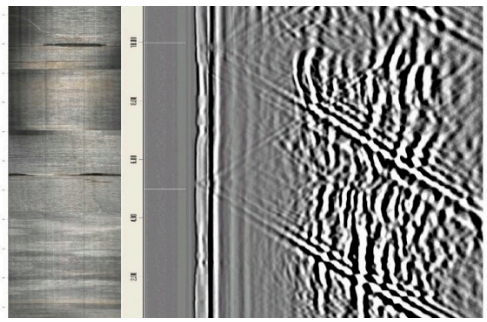

Figure 4. Comparison of GPR and optical imaging results in the same borehole.

Dielectric constant and wave velocity are the key parameters of GPR detection. The target depth method, the point source reflection method, and the Hough transform method are commonly used to estimate the dielectric constant. The known target depth method can estimate the dielectric constant quickly and easily, but the buried depth of a target in the detection region must be known. The Hough transformation method needs an accurate hyperbolic shape to estimate the dielectric

 doi:10.20944/preprints202603.2238.v1

constant. There is significant interference and noise in the echo, which will reduce the estimation accuracy. In addition, boreholes often pass through multiple formations, and the dielectric constants of each formation may vary greatly. Combining the results of borehole radar and borehole image, a new dielectric constant estimation method is proposed.

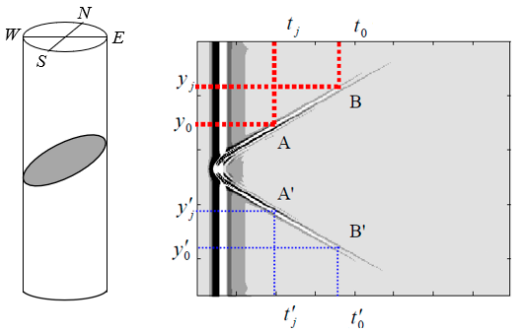

Figure 5. Schematic diagram of dielectric constant estimation based on borehole image and borehole GPR.

As shown in Figure 5, the borehole wall image and the radar time profile result image at the same position of the borehole are obtained. Firstly, the borehole image is analyzed, and the inclination and dip angle at the intersection of the structural plane and the borehole are calculated. Then, the contour of the target echo curve is extracted. The shape of the target echo curve is a function of the antenna moving position y, and the inclination ki of the curve is calculated using the following equation.

$$k_i = \frac{1}{m}\sum_{j=1}^{m}\left(y_j - y_0\right)/\left(t_j - t_0\right) \tag{1}$$

y_0 is the longitudinal coordinate of the reference position of the antenna, and t_0 is the two-way travel time of the radar wave detected at this time; y_j is the longitudinal coordinate of each detection point, and t_j is the two-way travel time of the radar wave; m is the number of sampling points. When the distance h between the antenna and the structural plane is much larger than the distance d between the transceiver antenna, the in-phase axis inclination of the radar range profile is as follows.

$$\beta_i' = \frac{\pi}{2} - \arctan\sqrt{2+2\cos 2\beta_i} \tag{2}$$

$$\tan\beta_i' = \frac{1}{m}\sum_{j=1}^{m}\left(y_j - y_0\right)/v_i\left(t_j - t_0\right) = k_i/v_i \tag{3}$$

$$v_i = k_i\sqrt{2+2\cos 2\beta_i} \tag{4}$$

k_i is the slope of the echo curve calculated by the fitting method; β_i is the inclination of the structural plane calculated by the digital hole wall image, and v_i is the calculated average wave velocity on the path between the hole and the target.

The relative dielectric constant of the rock-soil medium in the detection region ε_r is:

$$\varepsilon_r = \frac{c^2}{v_i^2} = \frac{c^2}{k_i^2\left(2+2\cos 2\beta_i\right)} \tag{5}$$

The relative dielectric constants calculated by combining the data of borehole radar and digital camera have the following characteristics: (1) The radar time profile image of the structural plane is open in the shape of scissors, and has upper and lower wings. If the upper and lower wings are symmetric about the horizontal axis, it indicates that the electromagnetic properties of the two sides of the structural plane are not very different. (2) When the slope of the curve of the upper and lower wings is different, it indicates that the dielectric constants of the two sides of the structural plane are

 doi:10.20944/preprints202603.2238.v1

different, and the value calculated by the upper wing is the geotechnical dielectric constant of the disk on the structural plane, while the value calculated by the lower wing is the geotechnical dielectric constant of the lower disk on the structural plane. (3) Because the borehole often passes through several formations, the permittivity of each formation may not be the same, but for two adjacent structural planes, the permittivity value calculated from the lower plate of the upper structural plane should be equal to the permittivity value calculated from the upper plate of the lower structural plane. (4) Since the structural plane is assumed to be a smooth plane during the derivation of this formula, the radar time profile obtained by actual detection is only applicable to the case where the upper and lower wings of the image are straight lines.

2.4. Dynamic Exploration Method of Geological Structures

Borehole GPR can receive the scattering echo on the abnormal body around the borehole in all directions, and the three-dimensional information is stored in the form of two-dimensional time series during data acquisition, the size and depth position of the abnormal body from the borehole axis can only be analyzed from the single hole radar data, but the azimuth information of the abnormal body cannot be determined. The borehole camera data can only identify the geological conditions around the borehole wall, including the strike and tendency of the fracture joint surface, and the distribution of the cavity area and karst area around the borehole wall. In order to quantitatively describe the distribution of abnormal geological bodies around the borehole, the multi-hole (at least two holes) data are required for joint analysis.

In order to determine whether there are karst, cavity and other unfavorable geological bodies in a certain area, dynamic survey technology will be an economical and efficient method. As shown in Figure 6, the first borehole A shall be selected near the site concerned (such as the foundation of a large bridge pier), and the drilling radar and digital camera shall be carried out according to the operation process of the dynamic survey technology to predict whether there is any unfavorable geological body that may cause safety hazards to the project in the site. If not, there is no need to increase the drilling work. If it is found that there may be unfavorable geological bodies in the site, but the location is unknown, Drilling and survey work shall be added. For example, the cavity detected in borehole A may be either in the concerned site or outside the site, so a borehole B needs to be added. When the cavity detected is far away from borehole B beyond the scope of the site, it means that the cavity measured in borehole A is not in the site, so the test work of the next borehole may not be added, or another borehole needs to be added, At this time, there are borehole radar and digital camera data in three boreholes, which can estimate the size and position of the abnormal body on the radar image to determine the impact on the project, so as to carry out reinforcement measures for subsequent projects.

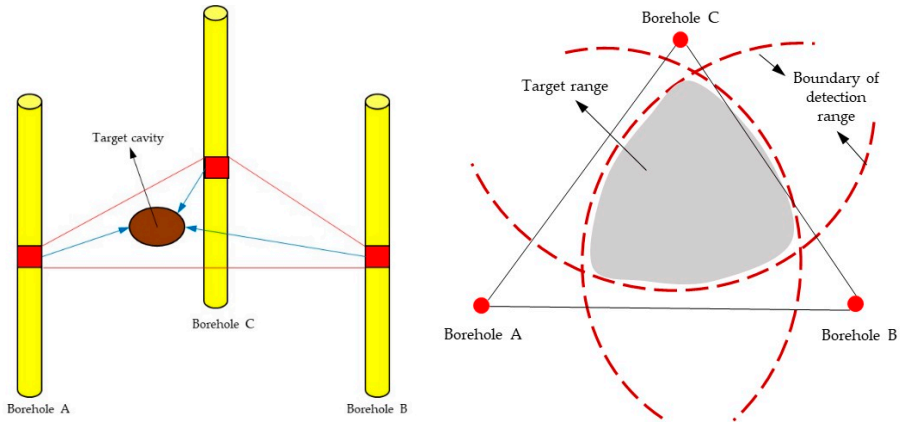

Figure 6. Sketch diagram of the dynamic exploration method.

Data fusion is a method of multivariate statistical joint analysis. For the analysis and research of the observed data of multiple holes, one approach is to analyze each hole separately, and the other is

 doi:10.20944/preprints202603.2238.v1

to analyze the multiple holes data at the same time. Although there are many uncertain factors in the underground abnormal geological body, the data from each hole still has a certain correlation. If they are processed separately, they will not only lose significant information, but it is often not easy to obtain good analysis results. Through the analysis of the observation data of multiple boreholes, we can study the relationship between the boreholes and reveal the inherent connectivity laws of these boreholes. Using different methods of multivariate analysis, we can also classify and simplify the geological anomaly bodies. As shown in Figure 7, there is only one obvious hyperbola at a certain depth on the single-hole radar profile. The electromagnetic wave propagation velocity in the stratum can be estimated using the method mentioned above, and the deviation size of the abnormal body can be calculated. As shown in Figure 5, at the same depth of the abnormal body, draw a circle with a radius of the distance from the drilling hole and the estimated size d of the target body in the drilling holes A, B, and C, respectively. By finding the joint area of the three arcs, you can find the approximate location of the abnormal body. This method can qualitatively and quantitatively describe the unfavorable geological bodies in the site through the digital camera and radar images of three boreholes, which is called the three-point survey method.

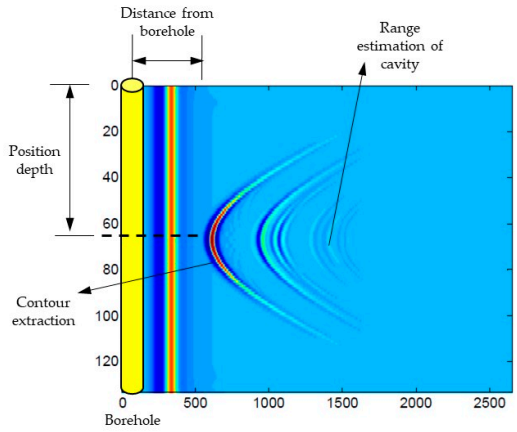

Figure 7. Extraction and estimation of borehole GPR echo curve.

The dynamic exploration methodology proposed in this study is defined as an adaptive drilling layout workflow based on phased information feedback. Its core principle involves iterative decision-making throughout the investigation process: after acquiring and rapidly analyzing borehole optical imaging and GPR data from an initial borehole (e.g., Borehole A), the exploration team evaluates whether additional boreholes (e.g., Boreholes B, C) are needed based on predefined anomaly identification criteria. These criteria include, but are not limited to: radar reflection amplitude exceeding a threshold (e.g., three times the background noise level), the estimated scale of the anomalous body (e.g., lateral extent > 2 m), and the spatial relationship between the anomaly and the engineering area of concern (e.g., distance to foundation footprint < 10 m). The primary objective of this adaptive approach is to efficiently and accurately delineate unfavorable geological bodies (such as fractures, karst cavities, or fracture zones) within the target area while minimizing the total number of boreholes required.

The field test process of the dynamic exploration method has been established, including the following:

(1) Mobilization: conduct an intermediate imaging survey on the boreholes at each control point. The result map of borehole photography can measure the integrity index of the rock core at the site, the formation fracture zone, and its dip angle, and even the possible corrosion area; At the same time, the existing drill holes are used for radar imaging in the hole, and the radar waveform profile is obtained to speculate the possible adverse geological phenomena within a range of tens of meters around.

 doi:10.20944/preprints202603.2238.v1

(2) Preliminary on-site analysis data: analyze the integrity of the site rock mass and whether there are adverse geological phenomena around the borehole according to the detection results of the control points.

(3) According to the results of preliminary analysis, if the single hole shows no obvious geological anomaly, it can directly enter the borehole of the next control point for testing; If abnormal geological bodies are found, additional boreholes can be drilled in the concerned area for multi-hole testing according to the actual needs of the project. Carry out joint test and analysis on two or more boreholes in the adjacent area. Based on digital borehole and radar profile images, the basic conditions of the structural planes between boreholes are mainly analyzed, such as the nature, occurrence, depth, and gap width of the structural planes, to distinguish the connectivity of the structural planes in different boreholes, and at the same time, the location, shape, and size of unfavorable geological bodies such as karst between boreholes can be accurately determined.

(4) The data shall be collated indoors, and the data of each hole shall be subject to correlation fusion analysis. The feature body shall be extracted through digital image analysis. The adverse geological structure shall be regression analyzed through the established geometric physical model to estimate the target size and location coordinates, to find out the geological conditions along the project more accurately, and complete the survey task.

3. Results

The Jinghu high-speed railway project is located in the eastern region of China, connecting Beijing and Shanghai. The Tengzhou section in Shandong Province was selected as the case study for several compelling reasons. First, this area features complex geological structures, including faults, folds, karst, and fracture zones, which provide an ideal setting to comprehensively validate the applicability and effectiveness of the proposed integrated detection method under challenging geological conditions. Specifically, the Tengzhou section lies within the western Shandong uplift area of the North China landmass, characterized by relatively complex tectonics. The Yishan fault divides the area into two parts: the western part is the Tengzhou fault depression, containing faults and anticlines of various directions and scales, while the eastern part forms the western edge of the pavilion fault depression. The regional strata are predominantly Cambrian and Ordovician of the Paleozoic era, with Carboniferous-Permian and Mesozoic Jurassic systems concealed beneath the widely developed Quaternary cover. The main engineering geological problems in this area include fracture zones, karst cavities, making it an excellent testbed for evaluating the proposed methodology.

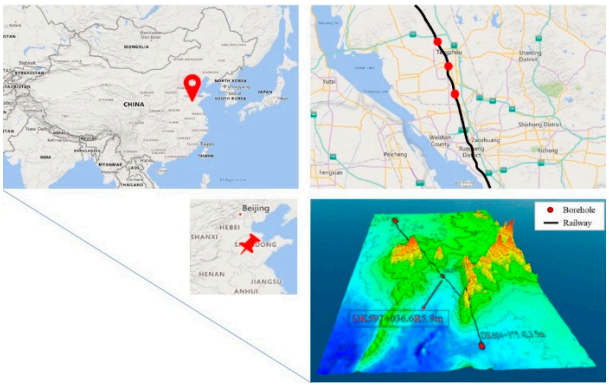

Figure 8. The geographical position of the Tengzhou Section of the Jinghu high-speed railway project.

The availability of high-quality data provides a solid foundation for method validation. A total of six boreholes were tested using both digital optical imaging and GPR in this survey, yielding comprehensive datasets for analysis. The test results from borehole optical imaging and borehole GPR were analyzed through data fusion. Figure 9 shows the comparison between the results of borehole optical imaging and borehole GPR, revealing numerous correlations between the two

 doi:10.20944/preprints202603.2238.v1

datasets. The optical images clearly reflect the occurrence of fractures on the borehole wall profile, while borehole GPR shows open scissors-like echo curves at corresponding depths, indicating the possible extension area of the cracks (Figure 9). The dielectric property contrasts between different media produce distinct radar echo characteristics, with aquifers and clay layers showing obvious absorption and attenuation effects on radar waves.

In addition, the availability of conventional drilling data in this area facilitates comparative analysis between our proposed method and traditional investigation results. The number of fractures can be determined from both borehole GPR and borehole optical imaging data. Due to the impact of drilling quality, evaluating rock mass integrity solely based on the RQD index from borehole coring or fracture counts from optical imaging may be inaccurate, as drilling disturbances can create new cracks around the borehole wall that might be misidentified as primary fractures. Borehole GPR can detect features within a range of more than ten meters around the borehole, thus reducing the impact of drilling-induced disturbances on integrity assessment. The number of fractures identified in borehole radar images is generally less than that in borehole optical imaging, as GPR results reflect the development degree of joint fissures in the rock mass surrounding the borehole wall. Therefore, for accurate evaluation of engineering rock mass integrity, it is necessary to integrate borehole GPR, borehole optical imaging, and borehole coring data.

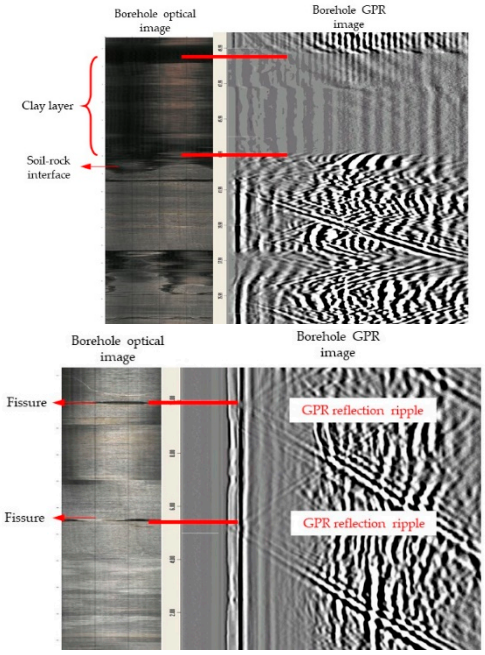

Figure 9. Reflection of geological characteristics in borehole optical images and borehole GPR.

Taking borehole DK597+036.6 as an example, shown in Figure 10, the borehole optical image and borehole GPR results show good consistency. At the 2m position, the optical image of the borehole shows a corrosion fissure with a width of about 50mm, and the borehole GPR results show energy attenuation. “Energy attenuation” refers to the relative weakening of reflected signal amplitudes observed in radar profiles, interpreted based on visual inspection and relative contrast. No absolute amplitude thresholds or quantitative signal-to-noise ratio calculations are defined. This descriptive usage aims to highlight the contrast between anomalous zones and the surrounding rock mass, rather than serving as quantitative signal analysis. Within the depth of 3.7-4.4m, the optical image of the borehole shows a cavity, and the borehole GPR results show an energy attenuation, with a certain extension along the borehole diameter. Within the depth of 6.5m-7m, the optical image of the borehole shows a fissure filled with mud, with a width of about 0.5m. The borehole GPR results show an energy attenuation zone with a width of 0.5m. Within the depth of 9.2-10m, the borehole image shows multiple fractures along calcite, and the borehole GPR results show multiple hyperbolic reflection zones. Within the depth of 13.1-15.6m, the optical image of the borehole shows karst

 doi:10.20944/preprints202603.2238.v1

limestone with developed karst fissures. The borehole GPR results show that the radar echo energy in this area is attenuated, and several hyperbolic reflection zones appear at some locations. At the location of 17.5m, the optical image of the borehole shows that there is a wide corrosion fissure, and the rock mass above and below the fissure has developed karst fissures. The borehole GPR results show that there is a wide hyperbolic reflection zone with energy attenuation. Within the range of 22.4-23.2m, the optical image of the borehole shows a corrosion area with multiple fractures interlaced. The borehole GPR results show energy attenuation with hyperbolic reflection. Within the range of 24.4-28.8m, the optical image of the borehole shows a large range of corroded limestone, accompanied by karst fissures and cavities. The borehole GPR results show that the energy is attenuated, and the energy in the radar echo reflection area is very weak. In this study, the dynamic survey technology based on borehole optical imaging and borehole radar was applied to the investigation project. By using a limited number of boreholes combined with advanced survey technologies, we accurately characterized the structural features of unfavorable geology, accelerated the project survey progress, reduced project costs, mitigated the hazards of unfavorable geology, and ensured the safety and stability of the foundation.

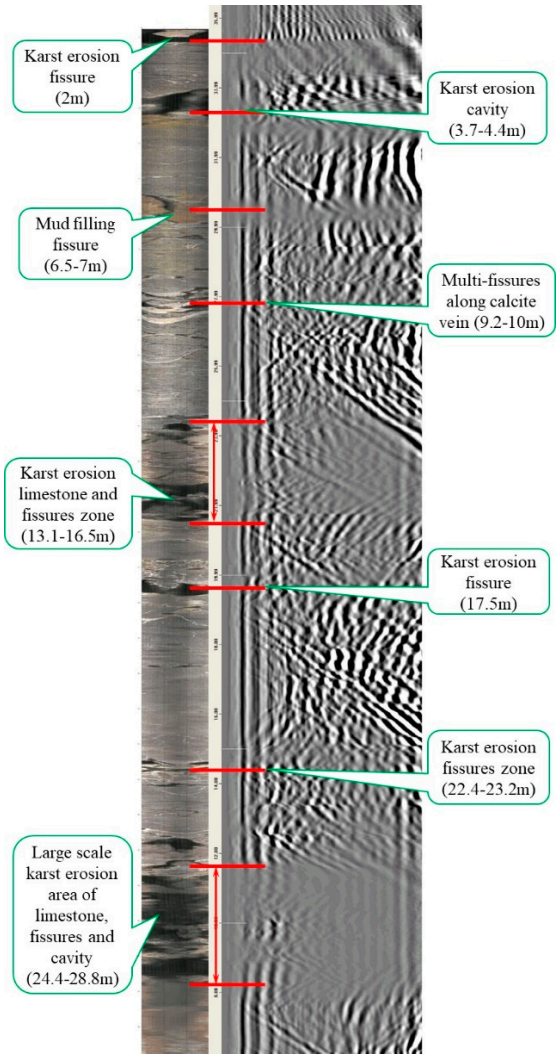

Figure 10. Comparison of borehole optical imaging and borehole GPR results (Borehole No. DK597+036.6).

It should be noted that the anomalous features identified in this section are primarily based on visual correlation between optical images and radar profiles, representing qualitative to semi-quantitative interpretation results. Due to the lack of independent validation data (e.g., verification through core drilling), rigorous statistical classification (such as confusion matrix analysis or false

 doi:10.20944/preprints202603.2238.v1

positive/false negative assessment) was not performed in this study. These features are presented to intuitively demonstrate the correlation patterns between the two methods, rather than serving as quantitative statistical indicators.

4. Discussion

The dynamic exploration methodology proposed in this study integrates borehole optical imaging and GPR within an adaptive drilling framework. While the method offers significant advantages in terms of reducing borehole numbers and improving investigation efficiency, it is important to acknowledge the inherent trade-off between sampling density and detection reliability. Reducing the number of boreholes inevitably increases the risk of missing subsurface anomalies that fall outside the detection range of the deployed boreholes, particularly for features with limited lateral extent or those located in areas not intersected by the adaptive drilling pattern.

This trade-off must be carefully managed in engineering practice. Based on our field experience and theoretical considerations, we recommend the following risk control strategies:

(1) For general exploration areas where geological conditions are relatively uniform or where the consequences of missing small-scale anomalies are acceptable, the full efficiency gains of the dynamic method can be realized by minimizing borehole counts. However, for critical engineering zones—such as major bridge pier foundations, tunnel portals, or areas with high seismic risk—a conservative approach with appropriate redundancy should be adopted. In such areas, we recommend maintaining at least one additional verification borehole even when preliminary data suggest no anomalies, or implementing a minimum borehole spacing criterion (e.g., no more than 20 m between boreholes) regard-less of dynamic feedback.

(2) The risk of detection omission can be partially mitigated by integrating complementary geophysical methods that provide different sensitivity patterns. For example, surface GPR or seismic refraction surveys can be deployed be-tween boreholes to screen for large-scale anomalies that might have been missed by the borehole-only approach. Any surface-detected anomalies can then be targeted for verification through additional boreholes.

(3) When implementing the dynamic decision-making workflow, we recommend incorporating safety margins into the stopping criteria. For instance, even if the predefined anomaly identification criteria are not met, drilling should continue until a minimum number of boreholes or a maximum borehole spacing threshold is achieved in critical areas.

(4) Future implementations of the dynamic method could benefit from incorporating a probabilistic framework that explicitly quantifies the detection omission probability as a function of borehole spacing, anomaly size distribution, and prior geological information. This would enable risk-informed decision-making where the acceptable level of detection omission risk is predefined based on project importance and consequence analysis.

It is important to clarify the intended scope of the proposed dielectric constant estimation method. While the simplified approach (Equations 1–5) enables rapid field screening, it relies on assumptions (planar reflectors, smooth structural planes, linear echo wings) that may not hold in heterogeneous fractured media. For high-precision applications requiring rigorous quantitative characterization, more advanced techniques such as full-waveform inversion (Ernst et al., 2007; Klotzsche et al., 2019) are recommended. Our method is positioned as a practical tool for preliminary assessment, providing approximate dielectric values to support velocity modeling and anomaly detection in engineering contexts where speed and cost efficiency are prioritized. This pragmatic trade-off aligns with the overall philosophy of the dynamic exploration approach: to deliver usable results with minimal borehole requirements while acknowledging the need for more sophisticated analysis when warranted.

Regarding the operational requirements, digital borehole optical imaging and borehole GPR are suitable for vertical and near-vertical drilling, and the borehole shall be smooth. Because the digital borehole camera system uses optical imaging technology, there is a certain requirement for the water clarity in the borehole. There is no application example of an optical system in very turbid water or a

 doi:10.20944/preprints202603.2238.v1

mud hole. If the water in the borehole is turbid, improvement measures must be taken, such as changing the water and washing the borehole to return clean water, alum precipitation, and standing. In addition, due to the use of mud to protect the wall in this geological survey, the hole was not washed away in time during the hole cleaning process, and the resulting image will have a certain impact. The improvement methods are as follows: (1) Drilling, digital camera, and geological radar comprehensive geological survey should be well coordinated; (2) For digital camera and borehole radar comprehensive survey, no matter how complex and unfavorable the underground rock and soil is, it is necessary to have basic measurable holes, so that the sensor probe can go deep into the ground and reach the required underground depth; (3) Digital borehole camera requires an aperture of Φ46-Φ130 mm, dry hole or clear water hole, and removal of the mud retaining wall; (4) Borehole radar requires an aperture greater than Φ50 mm.

While this study focuses primarily on geometric fracture characterization, we acknowledge that interpretations of fracture connectivity and potential hazard implications cannot be fully separated from the governing geomechanical framework. Although detailed mechanical analysis lies beyond our scope, we provide contextual discussion to bridge geometric observations and engineering risk. Fracture stability is inherently influenced by the ambient stress field, litho-logical contrasts, and fault-zone mechanics. In our study area—the tectonically complex western Shandong up-lift—fracture sets (e.g., steeply dipping fractures in borehole DK597+036.6) should be interpreted with consideration of regional stress patterns, even without direct measurements. Lithological interfaces between sandstone, limestone, and granite gneiss observed in borehole images correlate with enhanced fracture density, suggesting these boundaries war-rant attention in stability assessments. Furthermore, localized intense fracturing (e.g., the 24.4-28.8 m interval) may indicate proximity to larger-scale structural features where connectivity and permeability could be enhanced. We emphasize that our fracture observations serve as geometric inputs to risk assessment—highlighting areas for further investigation (stress measurements, permeability testing, numerical modeling)—rather than standalone stability indicators. Future research should integrate borehole imaging with in-situ stress characterization and hydro-mechanical modeling to transform these qualitative correlations into quantitatively robust inputs for engineering design.

As a final remark, we acknowledge that reproducibility is a fundamental scientific principle. While the current description of the data fusion framework provides sufficient practical detail for engineering application, we recognize that further standardization would enhance its quantitative rigor. Therefore, developing more standardized and quantitatively rigorous fusion protocols—including automated feature extraction algorithms, objective correlation criteria, and validated inversion strategies—represents an important direction for future research. Such advancements will help bridge the gap between conceptual methodology and fully reproducible analytical workflows, ultimately strengthening the scientific foundation of integrated borehole imaging techniques for engineering geological investigation.

5. Conclusions

This study has proposed a dynamic exploration methodology that integrates borehole optical imaging and GPR within an adaptive drilling framework, along with its fundamental principles and implementation workflow. The field application in the Tengzhou section of the Jinghu high-speed railway project demonstrates that the combined use of borehole radar and borehole optical imaging in geological exploration is effective. The fused analysis of processed bore-hole images and radar data provides an intuitive and comprehensive representation of rock morphology within the borehole, including key geological structural information such as the distribution of fractures, joints, and fracture zones. This successfully meets the goals of the dynamic survey approach.

The feasibility of this integrated method lies in its complementary strengths: optical imaging offers high-resolution, direct visual documentation of the borehole wall, capturing fine-scale discontinuities, while borehole GPR extends the investigation radially into the surrounding rock mass, detecting features beyond the borehole wall. The dynamic adjustment of survey layout—such

 doi:10.20944/preprints202603.2238.v1

as the triangular borehole pattern enables real-time refinement of exploration targets based on initial findings, thereby improving investigation efficiency and accuracy.

The dynamic exploration method demonstrates the ability to substantially reduce the number of boreholes while maintaining effective detection of fractures with apertures greater than 1 cm and meter-scale cavities. Integrated analysis of the six boreholes successfully identified common anomalous features, with good consistency between optical imaging and GPR results, validating the practical feasibility of the proposed approach.

In general, the preliminary exploration using the digital camera system and borehole geological radar in the high-speed railway project is successful. The processed borehole wall development map and three-dimensional visualization can clearly and accurately reflect the morphological characteristics of rocks in the borehole area, the distribution of fractures, joints, fracture zones, and the original state of geological structures such as rock veins. In particular, the three-hole survey method with triangular layout should be a recommended approach worth promoting.

Future applications of this methodology are promising, particularly in engineering projects requiring detailed sub-surface characterization, such as tunnel construction, dam foundation assessment, slope stability analysis, and mineral exploration. With ongoing advancements in sensor technology, data processing algorithms, and real-time interpretation software, the integration of borehole optical imaging and GPR is expected to become more automated, intuitive, and widely adopted. Furthermore, combining these datasets with machine learning techniques could enhance pattern recognition and predictive modeling of geological conditions, contributing to smarter and more risk-aware engineering design and construction. It is believed that more geological field investigations and comprehensive data analysis will lay a solid foundation for these technologies to better serve engineering practice in the future.

Funding: This research was funded by National Natural Science Foundation of China, grant number 42577215.

Data Availability Statement: The data presented in this study are available in the article.

Conflicts of Interest: The authors declare no conflicts of interest.

References

1. C. Y. Wang; X. R. Ge; S. W. Bai. Study of the digital panoramic borehole camera system. Chinese Journal of Rock Mechanics and Engineering. 2002, 21(3), pp. 398-403.
2. C. Y. Wang; Y. T. Wang; X. J. Zou; Z. Q. Han; S. Zhong. Study of a borehole panoramic stereopair imaging system. International Journal of Rock Mechanics and Mining Sciences. 2018, 104, pp. 174-181.
3. Z. Q. Han; C. Y. Wang; C. Wang; X. J. Zou; Y. Y. Jiao; S. Hu. A proposed method for determining in-situ stress from borehole breakout based on the borehole stereo-pair imaging technique. Journal of Rock Mechanics and Mining Sciences. 2018, 127, pp. 104215.
4. J. H. Kim; S. G. Park; M. J. Yi; et al. Borehole radar investigations for locating an ice ring formed by cryogenic conditions in an underground cavern. Journal of Applied Geophysics, 2007, 62(3), pp. 204-214.
5. Y. Yi; A. H. Johan; K. Anja; et al. Coupled full-waveform inversion of horizontal borehole ground penetrating radar data to estimate soil hydraulic parameters: A synthetic study. Journal of Hydrology, 2022, 610, pp. 127817.
6. J. C. Wang; H. H. Xu; J. P. Zou. Fine detection technology of rock mass structure based on borehole acousto-optic combined measurement. Measurement, 2022, 187, pp. 110259.
7. S. J. Li; X. T. Feng; C. Y. Wang; J. A. Hudson. ISRM Suggested method for rock fractures observations using a borehole digital optical televiewer. Rock Mechanics and Rock Engineering, 2013, 46(3), pp. 635-644.
8. J. C. Kavin. Application of ground-penetrating radar, digital optical borehole images, and cores for characterization of porosity, hydraulic conductivity, and paleokarst in the Biscayne aquifer, southeastern Florida, USA. Journal of Applied Geophysics, 2004, 55, pp. 61-76.
9. S. Zhong; C. Y. Wang; L. X. Wu; et al. Integrated application of borehole GPR and borehole imaging to geological surveys. Process in Geophysics, 2011, 26(1), pp. 335-341.

 doi:10.20944/preprints202603.2238.v1

10. T. Spillmann; H. Maurer; H. Willenberg; et al. Characterization of an unstable rock mass based on borehole logs and diverse borehole radar data. Journal of Applied Geophysics, 2007, 61(1), pp. 16-38.
11. J. H. Williams; C. D. Johnson. Acoustic and optical borehole-wall imaging for fractured-rock aquifer studies. Journal of Applied Geophysics, 2004, 55(1-2), pp. 151-159.
12. M. H. Serzu; E. T. Kozak; G. S. Lodha; et al. Use of borehole radar techniques to characterize fractured granitic bedrock at AECL's Underground Research Laboratory. Journal of Applied Geophysics, 2004, 55(1):137-150.
13. L. Li; R. Wang; T. Peng; et al. Identification of geo-bodies in borehole radar image based on Curvelet transform. Journal of Applied Geophysics, 2021, 189, pp. 104325.
14. X. J. Tang; T. Sun; Tang Z. J. Tang; et al. Geological disaster survey based on Curvelet transform with borehole Ground Penetrating Radar in Tonglushan old mine site. Journal of Environmental Sciences, 2011, 23(S), pp. 78-83.
15. Khamis M.; A. A. Basheer.Taha Rabeh et al. Geophysical assessment of the hydraulic property of the fracture systems around Lake Nasser, Egypt: In sight of polarimetric borehole radar. NRIAG Journal of Astronomy and Geophysics, 2014, 3(1). pp. 7-17.
16. C. Y. Jin; K. Wang; T. Han; et al. Segmentation of ore and waste rocks in borehole images using the multi-module densely connected U-net. Computers Geosciences, 2021, 159, pp. 105018.
17. Y. Yu; W. Lutz; K. Anja; et al. Sequential and Coupled Inversion of Horizontal Borehole Ground Penetrating Radar Data to Estimate Soil Hydraulic Properties at the Field Scale. Journal of Hydrology, 2021, 596, pp. 126010.
18. L. B. Liu. Virtual multi-offset reflection profiling with interferometric imaging for borehole radar—ScienceDirect. Signal Processing, 2017, 132, pp. 319-326.